Drawing Properties of Ultrahigh Molecular Weight Polyethylene Fibers Prepared at Varying Formation Temperatures

Jen-Taut Yeh,[1,2] Yue-Tang Lin,[2] Huang-Bin Jiang[2]

[1]*Institute of Chemistry and Material Science, Hubei University, Wuhan, China*
[2]*Graduate School of Fiber and Polymer Engineering, National Taiwan University of Science and Technology, Taipei, Taiwan*

Received 15 November 2002; accepted 11 June 2003

ABSTRACT: The values of the percentage crystallinity, melting temperature, birefringence, and cross-sectional area of ultrahigh molecular weight polyethylene (UHMWPE)/low MWPE (LMWPE) as-prepared fiber specimens are reduced consistently as the formation temperatures decreased from 60 to 0°C. Much more sparse structures with significantly larger voids are found on the fractured surfaces of those as-prepared fibers that were prepared at higher formation temperatures than those prepared at lower formation temperatures. The cross sections of the as-prepared fiber specimens gradually change from an oblate to a nearly circular to an uneven circular shape as the formation temperatures are reduced from 60 to 10 to 0°C, respectively. It is worth noting that the achievable draw ratios (D_{ra}) of the as-prepared fibers reach maximum when they are prepared at an optimum formation temperature of 10°C. Moreover, the D_{ra} values of the as-prepared fiber (UL_{10}) specimens can be further improved by using a two-stage drawing process, wherein the temperature used in the second drawing stage (T_{sec}) is higher than 95°C. In fact, the optimum T_{sec} of the two-stage drawn UL_{10} fiber specimens increases significantly from 105 to 115°C as the first-stage draw ratio (D_{lr}) values increase from 20 to 40, respectively. The birefringence values, tensile strengths, and moduli of one- and two-stage drawn UL_{10} fiber specimens increase consistently with increasing draw ratios, although the increasing rate of these values is gradually reduced as the draw ratios are greater than certain values. In contrast, at a constant draw ratio, the two-stage drawn UL_{10} fiber specimens drawn at a higher T_{sec} always exhibit higher values of birefringence, tensile strengths, and moduli than those with the same D_{lr} but drawn at a lower T_{sec}. Moreover, at a constant draw ratio, the birefringence values, tensile strengths, and moduli of the fiber specimens drawn at a fixed optimum T_{sec} reach the maximum when they are first drawn up to an optimum D_{lr} of about 50. In fact, by using the proper optimum T_{sec} and D_{lr}, the tensile strengths and moduli of the two-stage drawn UL_{10} fiber specimens can reach more than 11 and 155 GPa, respectively. The possible mechanisms accounting for these interesting properties are proposed in this study. © 2003 Wiley Periodicals, Inc. J Appl Polym Sci 91: 1559–1570, 2004

Key words: gel; formation temperatures; achievable draw ratios, first-stage draw ratio; optimum temperature

INTRODUCTION

The gel spinning of flexible polymers with relatively high molecular weights has attracted much attention for the last three decades, because of its availability in the production of high performance fibers. Polyethylene (PE),[1–2] polypropylene,[22,23] and poly(vinyl alcohol)[24–26] fibers are typical high performance fibers that are produced using the gel spinning process. Remarkable progress has been made in the improvement of these high performance fibers; however, the highest tensile strengths and moduli achieved for these fibers are still well below the broad range of theoretical tensile strengths and moduli reported for the perfect crystals of these polymers.[1] The highest tenacity of commercially available ultrahigh molecular weight PE (UHMWPE) fibers reaches 45 g/den, which is about 10 times higher than those of steel fibers.[5] However, this strength is still far below the theoretical achievable strength (372 g/den) reported for the perfect PE crystal.[21]

The key element in obtaining high strength and high modulus UHMWPE fibers is to find the way to ultradraw the gel fibers to an ultrahigh draw ratio after the gel spinning process. In fact, it was found that[7–15] the tensile strengths and moduli of the ultradrawn UHMWPE gel specimens improve consistently with increasing achievable draw ratios. Investigations[2,4,7–19] were performed to improve the achievable draw ratios and the corresponding tensile properties of UHMWPE gel specimens. The drawability of the gel specimens was found to depend significantly on the compositions of the solutions from which the gels were made.[6–14] The achievable drawability was reduced significantly when the gel films were prepared

Correspondence to: J.-T. Yeh (jyeh@hp730.tx.ntust.edu.tw)
Contract grant sponsor: National Science Council; contract grant numbers: NSC 88-2216-E011-028; 89-2216-E011-042; 90-2216-E011-032; 91-2216-E011-027.

from solutions whose concentrations deviated from their critical values, in which the numbers of entanglements in the coherent network structure of the gel films are too many or too few to yield the maximum extension of the UHMWPE during the gel-deformation processes.

By contrast, several authors[9,10,14,15,19,20] reported that the drawing temperature and rate could markedly affect the maximum achievable draw ratio of solution-grown UHMWPE samples. At a fixed drawing rate, the achievable draw ratios of film samples prepared from gel solutions of UHMWPE and low MWPE (LMWPE) blends were found to reach a maximum value when each film specimen was drawn at a temperature near its optimum temperature (T_{op}).[10,14–15] In fact, the T_{op} values of each film sample consistently increased with the drawing rate. The achievable draw ratio of each film sample drawn at a constant rate and at a temperature near T_{op} is referred to as the Dr_{aop}, which reached another maximum value as the drawing rates approached an optimum value. Moreover, the temperature dependence of the apparent elongational viscosity (η) revealed two distinguishable intervals with different activation energies (E_a). Coincidentally, the transition temperature (T_r) obtained from the intersection of two straight lines drawn parallel to two distinct intervals is approximately equal to the T_{op} value found for the film sample drawn at the same rate.[14,15] A dynamic mechanical analysis of the film samples exhibited an extraordinarily high α-transition peak at temperatures near 95°C, which are again very close to the T_{op} and T_r values found for the film samples drawn at varying rates; and they are significantly increased with the testing frequencies. Presumably, the two distinct deformation mechanisms and E_a values associated with the two distinct regions are due to the different molecular motions motivated in different temperature regions, wherein the molecular motions of the α transition of the film sample can only be activated in region 1.[15] However, in order to reduce the breakage of taut tie molecules before effectively pulling UHMWPE molecules out of the lamellar crystals at high deformation rates and to increase the achievable draw ratios of the film specimens, fast molecular motions and high drawing temperatures are required during the drawing process. Further, our recent investigations[11] found that the Dr_{aop} values of the gel films can be further improved by using a two-stage drawing process, in which the UHMWPE/LMWPE film specimens were drawn at another optimum temperature after they had been drawn at 95°C, up to a fixed draw ratio.

In addition to the gel solution compositions and drawing conditions, it is generally recognized that the conditions used in the formation process after spinning and/or solution casting of gel solutions can also have a significant influence on the morphology, microstructure, and drawing properties of the specimens formed during the above-mentioned processes.[2,14,27–34] We recently showed[14] that at any fixed drawing temperature, the critical draw ratios (D_{rc}) of UHMWPE/LMWPE film specimens prepared at varying formation temperatures were found to increase significantly as their formation temperatures (T_f) were reduced. In fact, by using an optimum drawing temperature of 95°C, the D_{rc} value of the UHMWPE/LMWPE specimen prepared at a 0°C formation temperature reach 488, which is about 50% higher than that of the specimen prepared at 95°C. Further investigations revealed that the UHMWPE/LMWPE specimens prepared at low T_f always exhibit a lower percentage of crystallinity, birefringence, and melting temperature than those prepared at higher T_f.

In this work, a systematic study of the influence of the formation temperature on the ultradrawing properties of UHMWPE/LMWPE fiber specimens is carried out. It is somewhat surprising that the dependence of their ultradrawing properties on the formation temperature is different from those film specimens prepared from UHMWPE/LMWPE gel solutions. The achievable draw ratios reached the maximum when the UHMWPE/LMWPE fiber specimens were prepared at an optimum formation temperature. Other investigations including surface morphology, birefringence, thermal, and tensile experiments were performed on the fiber specimens to further clarify the possible deformation mechanisms accounting for the interesting ultradrawing properties found for these fibers prepared at varying formation temperatures.

EXPERIMENTAL

Materials and sample preparation

The UHMWPE resin used in this study is associated with a weight-average molecular weight (M_w) of 4.5×10^6, which will be referred to as resin U in the following discussion. The LMWPE used in this study will be called resin L, which is a linear high density PE with a M_w of 9.0×10^4. Resins U and L were kindly supplied by Bruce Lu of Yung Chia Chemical Industrial Corporation (Kaohsiung, Taiwan). The U and L were mixed at a weight ratio of 98:2 and then dissolved in decalin at 150°C for 4 h, and 0.1 wt % di-*t*-butyl-*p*-cresol was added as an antioxidant. These gel solutions were then fed into a temperature-controlled hopper and kept as hot homogenized solutions before further spinning. The prepared solutions were then gel spun using a conical die with an exit diameter of 1 mm at 150°C and an extrusion rate of 3000 mm/min. A water bath and a winder with a 70-mm diameter were placed at distances of 200 and 650 mm from the spinneret exit, respectively. The extruded gel fibers were cooled in an air-conditioned atmosphere and then quenched into a water bath for about 1 min; the temperatures of the air atmosphere and water bath were controlled at 0, 5, 10, 15, 20, and 60°C, respectively. The quenched fibers were then extracted in an *n*-hexane bath for 5 min to remove the residual decalin

TABLE I
Compositions of Gel Solutions of UHMWPE/LMWPE Blends

Sample	Weight ratio (UHMWPE/LMWPE)	Formation temp. (°C)
UL_0	98/2	0
UL_5	98/2	5
UL_{10}	98/2	10
UL_{15}	98/2	15
UL_{20}	98/2	20
UL_{40}	98/2	40
UL_{60}	98/2	60

solvent. The extracted fiber specimens were dried in air for 30 min to remove the remaining hexane solvent before any drawing runs. The compositions of the gel fibers prepared in this study are summarized in Table I.

Morphology, birefringence, and thermal analysis

In order to observe the morphology of the as-prepared and drawn gel fibers prepared under varying conditions, the fibers were immersed and fractured in a liquid nitrogen atmosphere. The fractured samples were gold coated and examined using a Jeol JSM-5200 scanning electron microscope. The birefringence properties of the as-prepared and drawn gel fibers were measured using a polarizing microspectrometer (model TFM-120 AFT). The thermal analysis of the behavior of all samples was performed on a DuPont differential scanning calorimeter (DSC No model 2000). All scans were carried out at a heating rate of 10°C/min under flowing nitrogen at a flow rate of 25 mL/min. Samples weighing 0.5 and 10 mg were placed in standard aluminum sample pans for determination of their melting temperatures and percentage of crystallinity. The percentage of crystallinity values of the specimens were estimated using baselines drawn from 40 to 170°C and a perfect heat of fusion for PE of 293 J/g.[35]

One- and two-stage drawing and tensile experiments

The fiber specimens used in the one- and two-stage drawing experiments were cut from the dried as-prepared fibers and then stretched on a Tensilon testing machine (model RTA-1T) equipped with a temperature-controlled oven at a crosshead speed of 20 mm/min. The fiber specimens (30-mm length) were first drawn at 95°C to a draw ratio of 10, 20, 40, 60, 80, and 100, respectively. These drawn fiber specimens were then further drawn at 105, 115, and 125°C. This type of drawing experiment is referred to as the two-stage drawing process in the following discussion. The draw ratio of each fiber specimen was determined as the ratio of the marked displacement before and after drawing. For purposes of comparison, the fiber specimens were also drawn at 95°C with varying draw ratios at a crosshead speed of 20 mm/min. This type of drawing experiment is referred to as the one-stage drawing process. The marked displacement before drawing was 27 mm. The tensile properties of the one- and two-stage drawn fiber specimens were also determined using the Tensilon testing machine at 28°C and a crosshead speed of 20 mm/min.

RESULTS AND DISCUSSION

Thermal, and birefringence properties and surface morphology of fibers prepared at varying formation temperatures

Typical DSC thermograms and percentage of crystallinity (X_c) values of the fibers prepared with varying formation temperatures are summarized in Figure 1. It is interesting to note that the values of the percentage of crystallinity and melting temperature of the as-prepared fibers decrease significantly as their formation temperatures are reduced. As shown in Figure 1, the respective crystallinity values and melting temperatures decrease from 78.4% and 137.6°C to 75.4% and 136.8°C to 71.3% and 136.1°C as the formation tem-

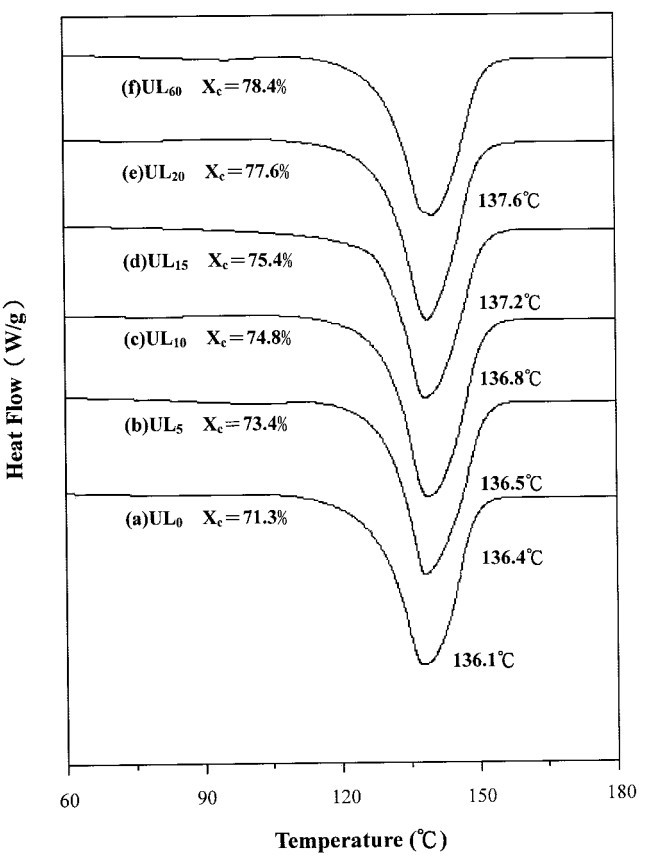

Figure 1 DSC thermograms of (a) UL_0, (b) UL_5, (c) UL_{10}, (d) UL_{15}, (e) UL_{20}, and (f) UL_{60} as-prepared fibers (X_c, the percentage crystallinity values of the as-prepared fibers).

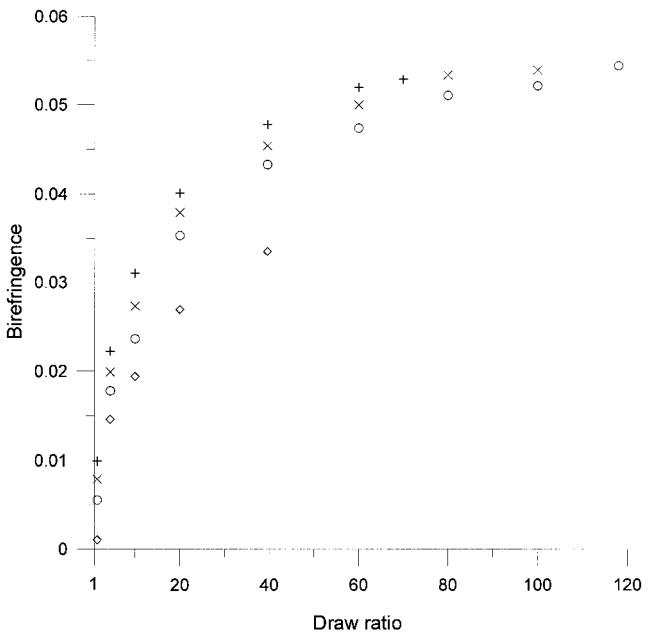

Figure 2 The birefringence of varying draw ratios for (◇) UL_0, (○) UL_{10}, (×) UL_{20}, and (+) UL_{60} fibers drawn at 95°C.

peratures of the as-prepared fibers decrease from 60 to 15 to 0°C, respectively. The typical birefringence values of the fibers prepared at varying formation temperatures are summarized in Figure 2. Note that the birefringence values of the fiber specimens prepared at higher formation temperatures were always higher than those of specimens prepared at lower formation temperatures. For instance, the birefringence values of UL_{60} fiber specimens are about 10, 20, and 40% higher than those of UL_{20}, UL_{10}, and UL_0 fiber specimens, respectively.

Figure 3 exhibits the typical cross-sectional shape of the fibers prepared with different formation temperatures. As expected, the cross sections of the as-prepared fibers was consistently reduced as their formation temperatures were reduced from 60 to 0°C. However, it is worth noting that an oblate-shaped cross section was found when the fibers were prepared at a relatively high formation temperature of 60°C (i.e., the UL_{60} fiber specimen). In contrast, the cross-sectional shapes of the fibers change significantly as the formation temperatures are reduced from 60 to 0°C. The cross section of the as-prepared fiber specimens then gradually changed from oblate to nearly circular as the formation temperature was reduced to about 10°C (i.e., the UL_{10} fibers). However, the surfaces of the UL_0 fiber prepared at a 0°C formation temperature appear to shrink significantly and have more "folded wrinkles" than those of UL_{10} fibers. As shown in Figure 3(a), the folded wrinkles squeezed and changed the cross section of UL_0 into an uneven circular shape compared to that of UL_{10}. Figure 4 exhibits a higher magnification of the cross-sectional surface morphology of the fibers prepared at varying formation temperatures. There were many more sparse structures with significantly larger voids that were found on the fractured surface of the fibers prepared at higher formation temperatures than those prepared at lower formation temperatures. Further investigations indicated that a clear skin–core morphology was found on the edge of the cross section of the fibers prepared at various formation temperatures. In fact, as shown in Figure 4(a–c), a clearly defined skin morphology was found on the edge and/or folded wrinkles of the cross section of the fibers prepared at lower formation temperatures than those prepared at higher temperatures.

It is not completely clear what causes the interesting thermal and birefringence properties and surface morphology described above. However, it is generally recognized that the crystallization temperature can have a significant influence on the crystallization kinetics and crystalline morphology of polymers. Several investigations[36–42] indicate that crystals obtained at low crystallization temperatures have a low degree of perfection and that these crystals can partially melt and recrystallize during the course of thermal analysis scans to yield thicker and/or more perfect crystals. Based on these premises, it is reasonable to believe that the low values for the percentage of crystallinity, birefringence, and melting temperature found for fiber specimens prepared at low formation temperatures are attributable to their low formation and/or crystallization temperatures, because the mobility of the UHMWPE molecules is expected to be reduced with decreasing temperatures, which can inhibit the crystallization and orientation of UHMWPE molecules at low formation and/or crystallization temperatures. In contrast, during the solvent vaporization and extraction processes, the higher mobility of UHMWPE molecules present in the as-spun fibers prepared at higher formation temperatures can help the UHMWPE molecules coagulate more easily than those of as-spun fibers prepared at lower formation temperatures, hence causing significantly larger void, and more sparse structure morphology on the fractured surfaces of as-prepared fibers prepared at higher formation temperatures. Moreover, after contacting the as-spun fibers with the roller during the extracting and cooling processes, the higher mobility of UHMWPE molecules present in the fibers prepared at higher formation temperatures can help reshape the circular cross section of the fibers into an oblate shape more easily than those of the fibers prepared at lower formation temperatures. The cross section of the as-prepared fiber specimens then gradually changed from oblate to nearly circular as the formation temperature was reduced to about 10°C. The as-spun fibers are expected to cool faster, shrink more, and exhibit thicker and/or more clearly defined skin morphology as their formation temperatures decrease. However, the more clearly defined skin morphology can cause the fiber specimens to shrink unevenly, because the density of

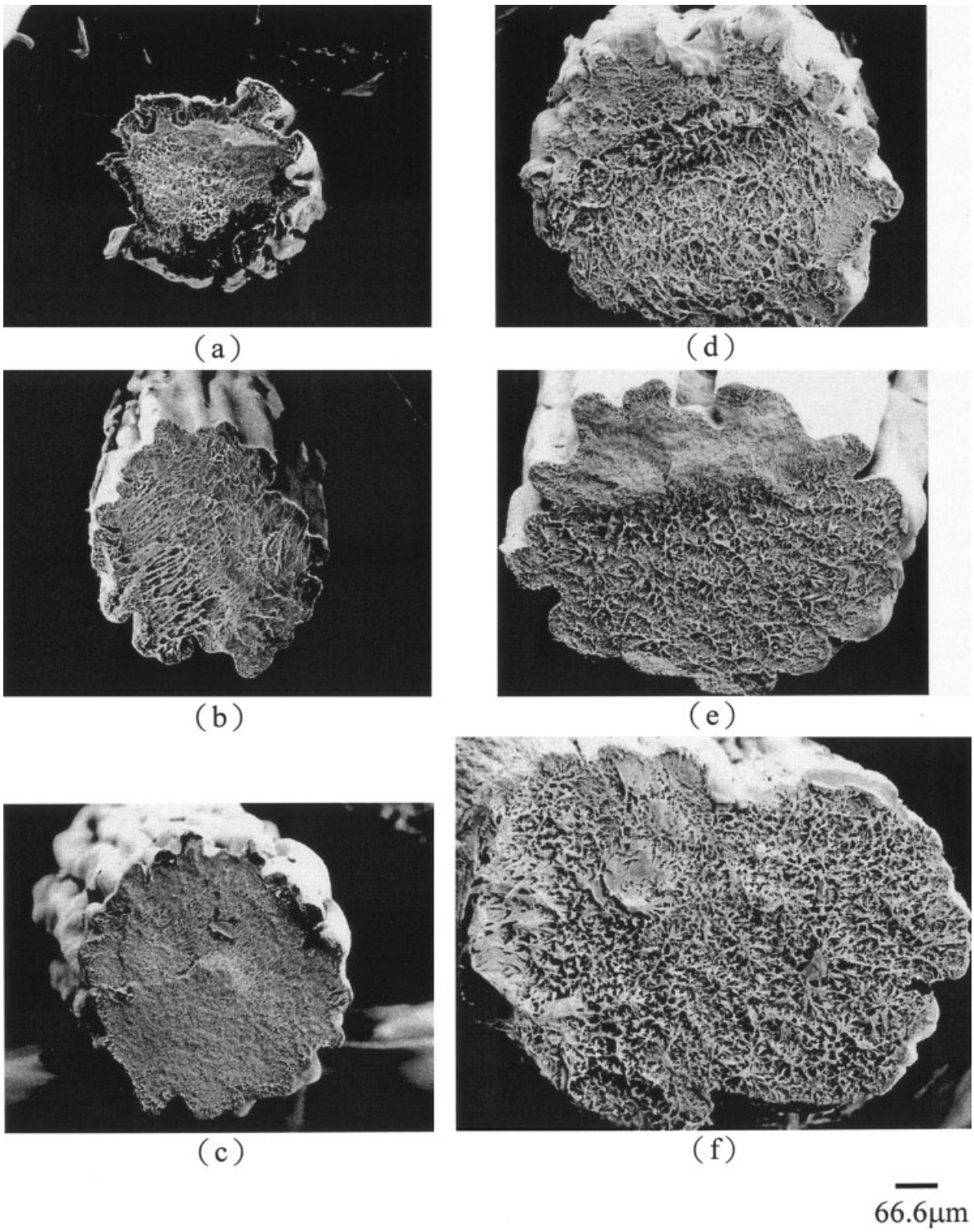

Figure 3 Scanning electron micrographs of the cross-sectional shapes of (a) UL_0, (b) UL_5, (c) UL_{10}, (d) UL_{15}, (e) UL_{20}, and (f) UL_{60} as-prepared fiber specimens.

the core structure is generally recognized to be larger than that of the skin structure of as-prepared fibers. As a consequence, uneven cross-sectional shapes with significantly folded wrinkles were found for the as-prepared fibers with formation temperatures less than the optimum of 10°C.

Drawing properties of one-stage drawn as-prepared fibers

Figure 5 exhibits the formation temperature dependence of the achievable draw ratios (D_{ra}) of as-prepared fibers drawn at 95°C. It is worth noting that the D_{ra} values of these fibers increased consistently from

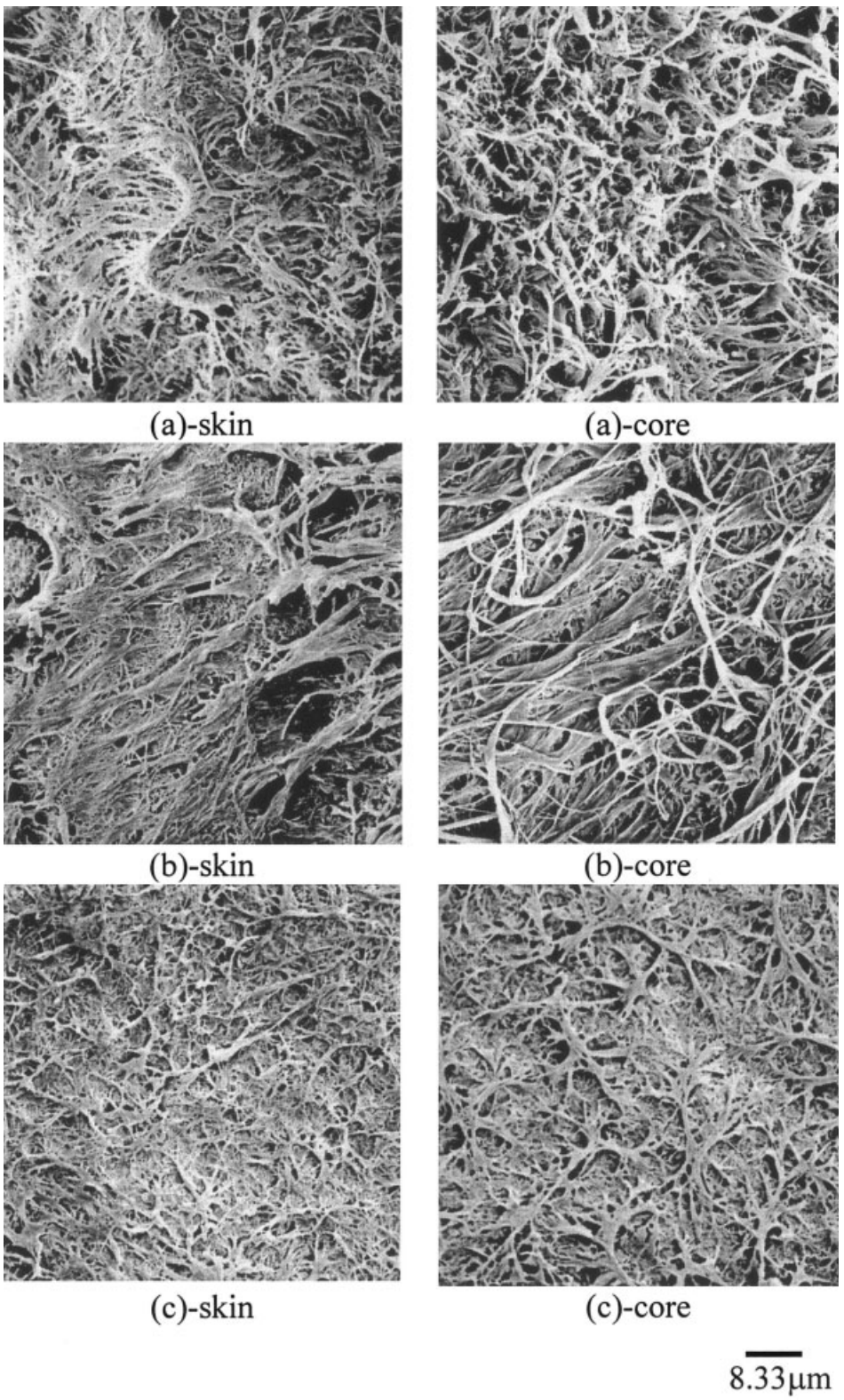

Figure 4 The skin–core morphology of the cross section of (a) UL_0, (b) UL_5, (c) UL_{10}, (d) UL_{15}, (e) UL_{20}, and (f) UL_{60} as-prepared fiber specimens.

75 to 126 as their formation temperatures were decreased from 60 to 10°C. Somewhat surprisingly, the D_{ra} values of the fibers then decreased significantly from 126 to 94 to 41 as the formation temperatures were reduced from 10 to 5 to 0°C, respectively. The factors that account for the interesting drawing properties of these fibers are not completely clear. However, in addition to the microstructure present in the

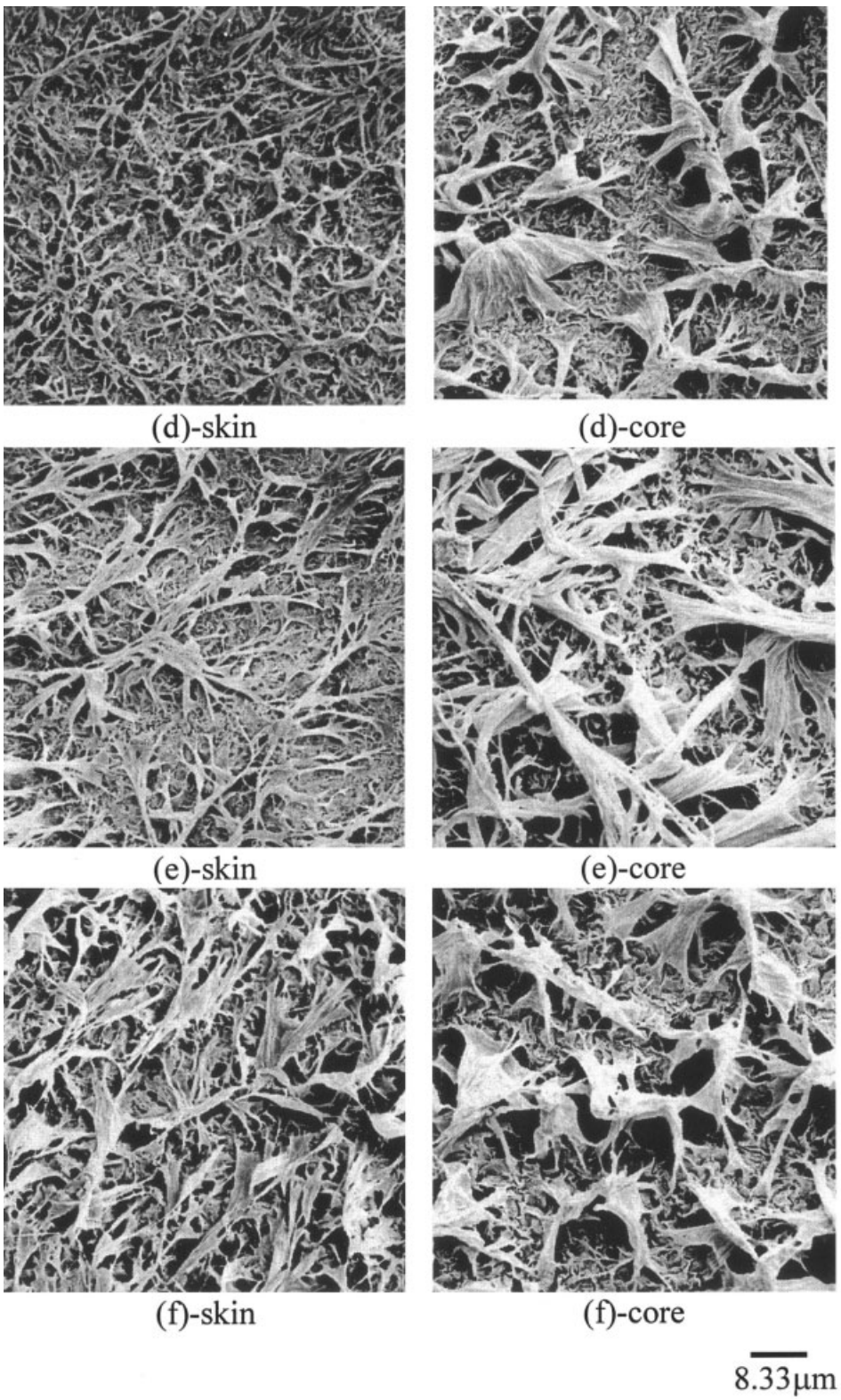

Figure 4 (*Continued from the previous page*)

as-prepared fibers, the uniformity and the shape of the cross section of the fibers can have a significant influence on their drawability. In contrast to a circular cross section, irregular fiber cross sections can easily cause stress concentration and early breakage of as-prepared fibers during the drawing processes, hence significantly reducing their drawability during the ultra-drawing process of fibers. As described in the previous section, the shape of the cross section of the as-prepared fibers changed from oblate to nearly

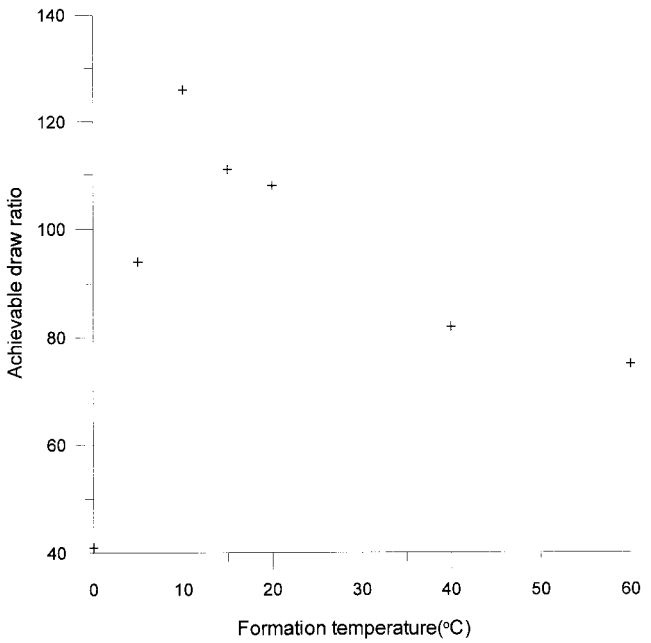

Figure 5 The achievable draw ratios of as-prepared fibers prepared at varying formation temperatures and drawn at 95°C.

symmetrical circular as the formation temperatures were reduced from 60 to 10°C. In addition, the percentage of crystallinity, birefringence, and melting temperature of these fibers decreased consistently as their formation temperatures were reduced. Presumably, during the ultradrawing processes, the more symmetrical circular cross sections, less perfect crystals, and oriented structures of as-prepared fibers prepared at lower formation temperatures can be more easily melted, disentangled, unfolded, and effectively pulled out of folded lamellar crystals without a significant stress concentration than those of fibers prepared at higher formation temperatures. Thus, their drawability is significantly improved as their formation temperatures were reduced from 60 to 10°C. However, the uneven circular cross section with demarcated folded wrinkles found on the surfaces of the as-prepared fibers with preparation temperatures lower than 10°C (i.e., the UL_0 and UL_5 as-prepared fibers) can cause significant stress concentration and early breakage of the as-prepared fibers during the drawing process, although they are associated with being more easily melted, disentangled, and unfolded structures. As a consequence, the one-stage achievable draw ratios reach the maximum as the formation temperatures of the as-prepared fibers reach the optimum temperature of 10°C.

Drawing properties of two-stage drawn UL_{10} fibers

The typical effects of the drawing conditions on the D_{ra} values of two-stage drawn fibers are shown in Figure 6. It is interesting to note that, after drawing UL_{10} specimens at 95°C up to fixed first-stage draw ratios (D_{lr}) ranging from 10 to 20, the D_{ra} values of the two-stage drawn UL_{10} specimens can be further improved by drawing the specimens in the second stage at an optimum temperature of about 105°C. The D_{ra} values of the two-stage drawn UL_{10} specimens then decreases significantly as the temperatures used in the second drawing stage (T_{sec}) increase to 115 and 125°C. A similar optimum T_{sec} was found for other two-stage drawn UL_{10} specimens with different first-stage draw ratios. In fact, the optimum T_{sec} of two-stage drawn UL_{10} increased significantly with the increasing D_{lr}. Figure 6 shows that the optimum T_{sec} increased from 105 to 115°C as the D_{lr} values of the UL_{10} specimens increased from 20 to 40, respectively. The D_{ra} values obtained for the two-stage UL_{10} specimens drawn at the optimum T_{sec} will be referred to as the optimum achievable draw ratio (D_{raopm}) in the following discussion. As shown in Figure 7, it is worth noting that the D_{raopm} values of the two-stage drawn UL_{10} fiber specimens increased consistently with increasing D_{lr} values until reached about 50. In contrast, the values of D_{raopm} were reduced significantly to 141 and 128 after UL_{10} specimens were first drawn to the draw ratios of 80 and 100, respectively at 95°C. Finally, it is important to note that the D_{raopm} value of two-stage drawn UL_{10} can be 27% higher (160 vs. 126) than the maximum D_{ra} obtained by drawing the UL_{10} as-prepared fiber specimen using the optimum one-stage drawing temperature of 95°C. These results clearly suggest that the D_{raopm} values of the two-stage drawn fiber specimens can be further improved so that they are higher

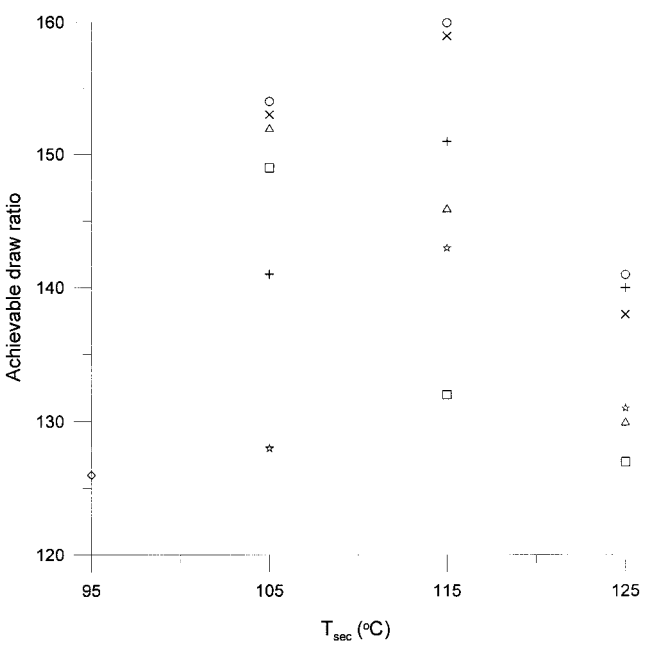

Figure 6 The achievable draw ratios of (◇) one and two-stage drawn UL_{10} fiber specimens at varying T_{sec} and with a D_{lr} of (□) 10, (△) 20, (×) 40, (○) 50, (+) 80, and (☆) 100.

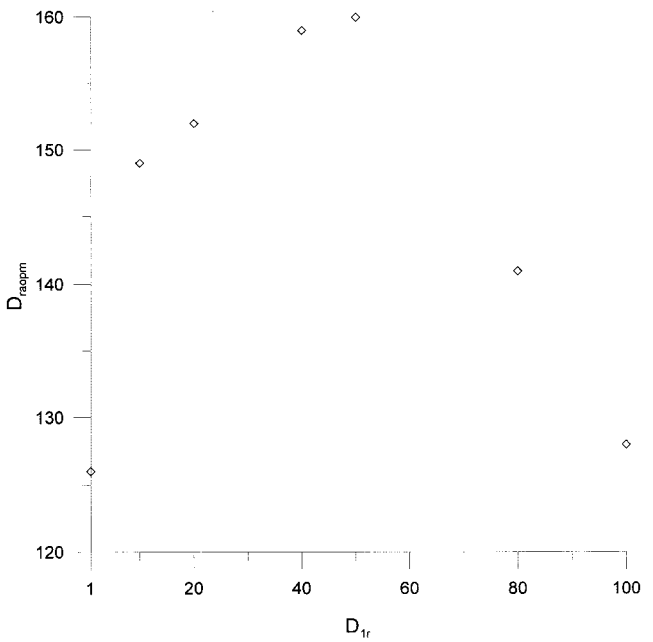

Figure 7 The D_{raopm} values of two-stage drawn UL_{10} fiber specimens with varying D_{lr}.

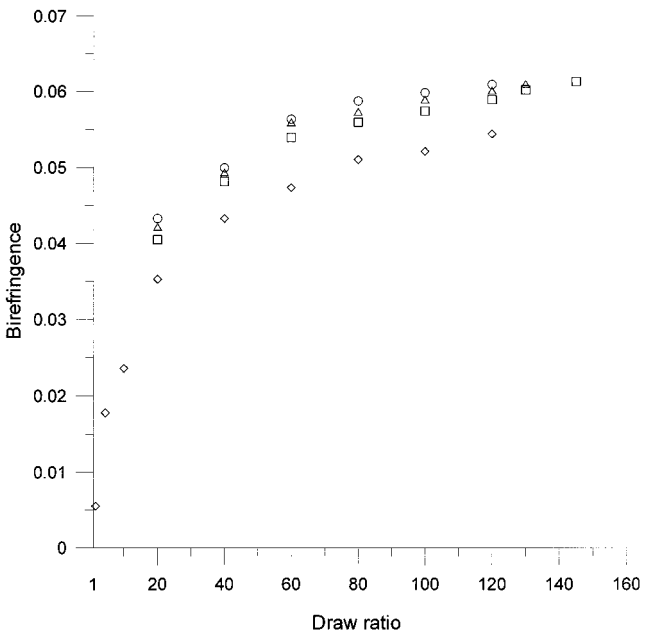

Figure 8 The birefringence values of varying draw ratios of (◇) one-and two-stage drawn UL_{10} fiber specimens with a D_{lr} of 10 and drawn at (□) 105, (△) 115, and (○) 125°C.

than those of the corresponding one-stage drawn fiber specimens, as T_{sec} and D_{lr} are adjusted to their optimum values.

Birefringence properties of one- and two-stage drawn UL_{10} fibers

The typical birefringence values of one- and two-stage drawn UL_{10} fibers are shown in Figures 8–10. Similar to those found in our previous studies,[8–14] the birefringence values of one- and two-stage drawn UL_{10} specimens are initially dramatically increased with an increasing draw ratio. The increasing rate of birefringence (IRB) becomes slower when the draw ratios of the drawn fibers are greater than about 10. In fact, the IRB consistently decreases with the increasing draw ratio until its value reaches about 80. After this value, the IRB remains approximately constant with the increasing draw ratio. However, it is worth noting that, at a fixed draw ratio, the two-stage drawn UL_{10} specimens drawn at a higher T_{sec} always exhibit higher values of birefringence than those with the same D_{lr} but drawn at a lower T_{sec}. Presumably, this can be due to the higher mobility of the UHMWPE molecules at higher temperatures such that the UHMWPE molecules present in the UL_{10} specimens can be more easily oriented along the drawing direction during the second drawing stage. However, it is not completely clear why the IRB is consistently reduced as the draw ratio increases from about 10 to 80, and it remains approximately constant when the draw ratios of the drawn UL_{10} fibers are higher than 80 or lower than 10. Figure 11 summarizes the birefringence values of two-stage drawn UL_{10} fiber specimens drawn at their optimum T_{sec}. We found it somewhat interesting that, at a fixed draw ratio, the birefringence values of the fiber specimens drawn at a fixed optimum T_{sec} increase consistently with an increasing D_{lr} until its value reaches about 50. The birefringence values then are significantly reduced as D_{lr} reaches 80. For example, after

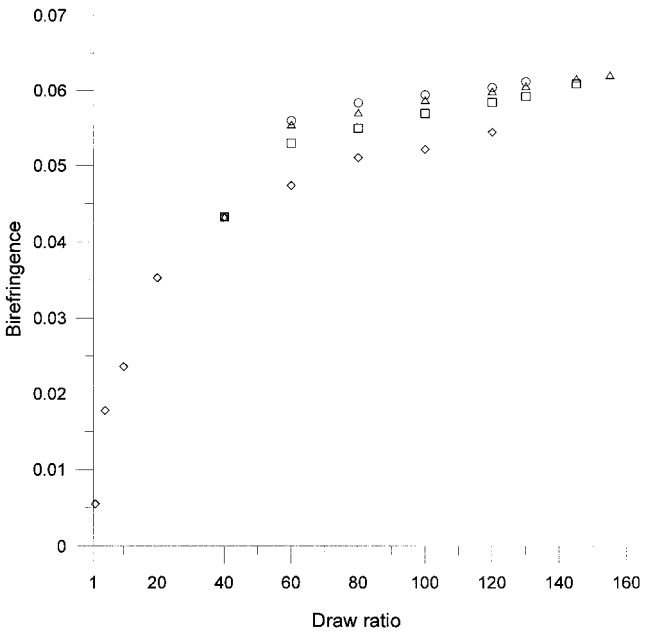

Figure 9 The birefringence values of varying draw ratios of (◇) one-and two-stage drawn UL_{10} fiber specimens with a D_{lr} of 40 and drawn at (□) 105, (△) 115, and (○) 125°C.

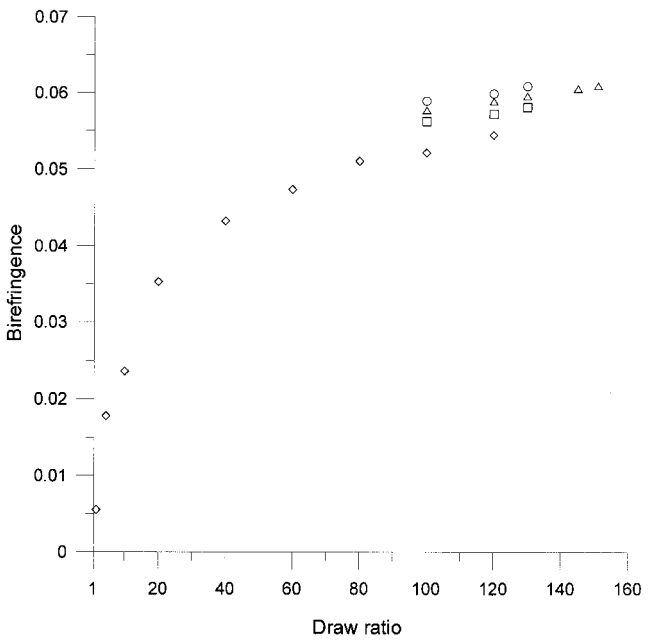

Figure 10 The birefringence values of varying draw ratios of (◇) one-and two-stage drawn UL_{10} fiber specimens with a D_{lr} of 80 and drawn at (□) 105, (△) 115, and (○) 125°C.

drawing the UL_{10} specimen up to a draw ratio of 50 at 95°C, the birefringence value of the two-stage drawn UL_{10} specimen with a draw ratio of 100 or 120 is about 5–10% higher than those of the one- and two-stage drawn gel specimens with D_{lr} values other than 50.

Tensile properties of one- and two-stage drawn UL_{10} fibers

Similar to the improvement in the birefringence properties, the tensile strengths and moduli of one- and two-stage drawn UL_{10} fiber specimens drawn at their optimum T_{sec} were found to improve dramatically with increasing initial draw ratios (see Figs. 12, 13). The increasing rates of the tensile strengths and moduli were then reduced significantly with further increases in the draw ratios. At even higher draw ratios (say 80), the increasing rates of the tensile strengths and moduli then remained relatively constant with increasing draw ratios. Most interestingly, at a fixed draw ratio, the tensile strengths and moduli of the two-stage drawn as-prepared fibers drawn at their optimum T_{sec} were also found to improve substantially as D_{lr} was increased to its optimum value of 50 (see Figs. 12, 13). It is generally believed that the mechanical properties of drawn fibers mainly depend on the degree of orientation of the drawn fiber specimens, as long as their molecular weights are constant. As mentioned previously, the degree of orientation and/or birefringence, tensile strength, and moduli of the two-stage drawn UL_{10} fibers all exhibited a similar dependence on the draw ratio. Moreover, at a fixed draw ratio the degree of orientation and/or birefringence improved consistently with increasing T_{sec} and D_{lr} until T_{sec} and D_{lr} were increased to their optimum values. These results suggest that good orientation of UHMWPE molecules along the drawing direction has a beneficial influence on the tensile strengths and moduli of fiber specimens, which can be obtained by drawing the fiber specimens using their corresponding optimum T_{sec} and D_{lr}. In fact, by using the proper optimum T_{sec} and D_{lr}, the tensile strengths and moduli of the two-stage drawn UL_{10} specimen can reach more than 11 and 155 GPa, respectively.

CONCLUSIONS

The percentage of crystallinity, melting temperature, birefringence, and cross-sectional area of the as-prepared fiber specimens were consistently reduced as the formation temperatures were decreased from 60 to 0°C. Much more sparse structures with significantly larger voids were found on the fractured surfaces of fibers prepared at higher T_f than those prepared at lower T_f. The cross section of the specimens gradually changed from oblate to nearly circular as the formation temperatures were reduced from 60°C to about 10°C. However, the cross-sectional shape changed into an uneven circular shape as their T_f values were reduced to less than 10°C. Further investigations indicated that a demarcated skin–core morphology and folded wrinkles were present on the edge of the cross section of UL_0 and UL_5 as-prepared specimens. Presumably, the clearly defined skin morphology can cause the fiber specimens to shrink unevenly at rela-

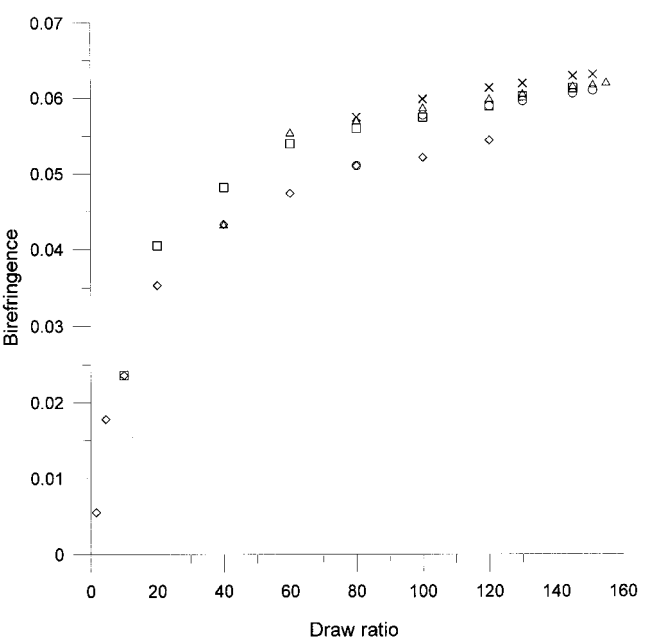

Figure 11 The birefringence values of varying draw ratios of (◇) one-and two-stage drawn UL_{10} fiber specimens with a D_{lr} of (□) 10, (△) 40, (×) 50, and (○) 80 and drawn at their optimum T_{sec}.

tively low T_f, because the density of the core structure is generally recognized to be larger than that of the skin structure of as-prepared fibers. It is worth noting that the achievable draw ratios of these fibers reached the maximum when they were prepared at an optimum formation temperature of 10°C. Presumably, during the ultradrawing processes, the more symmetrical circular cross section, less perfect crystals, and oriented structures of the fibers prepared at lower T_f can be more easily melted, disentangled, unfolded, and effectively pulled out of folded lamellar crystals without significant stress concentration than those of fibers prepared at higher temperatures. However, the uneven circular cross section with demarcated folded wrinkles found on the surfaces of the UL_0 and UL_5 specimens can cause significant stress concentration and early breakage of the specimens during the drawing process, although they are associated with being more easily melted, disentangled, and unfolded structures. As a consequence, the one-stage achievable draw ratios reach the maximum as the formation temperatures of the as-prepared fibers reach the optimum temperature of 10°C. In contrast, after drawing the fiber specimens at 95°C up to fixed first-stage draw ratios ranging from 10 to 80, the D_{ra} values of the two-stage drawn UL_{10} fiber specimens can be further improved by drawing the specimens in the second stage at an optimum T_{sec}. In fact, the optimum T_{sec} of the two-stage drawn UL_{10} fibers increased significantly from 105 to 115°C as the D_{lr} values were increased from 20 to 40, respectively. It is important to note that the D_{ra} of the two-stage drawn UL_{10} specimens can be further improved to 27% higher than those of the corresponding one-stage drawn specimens as the T_{sec} and D_{lr} are adjusted to their optimum values.

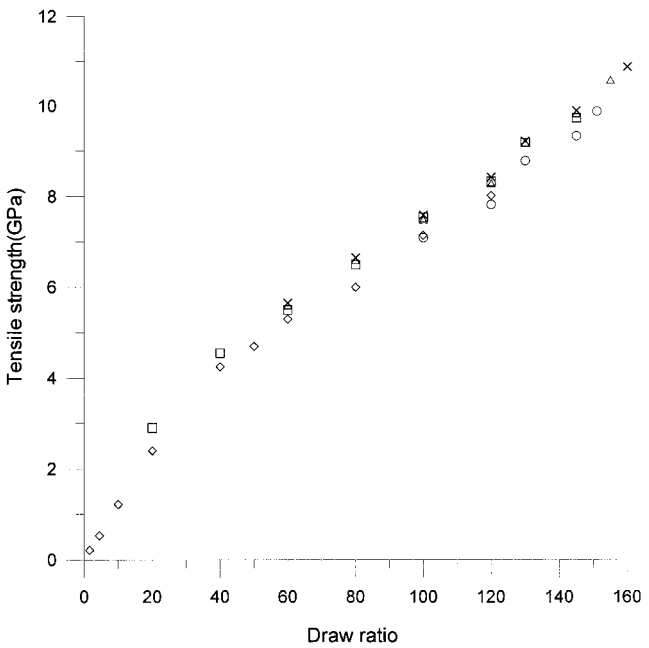

Figure 12 The tensile strengths of (◇) one- and two-stage drawn UL_{10} fiber specimens drawn at their optimum T_{sec} with a D_{lr} of (□) 10, (△) 40, (×) 50, and (○) 80.

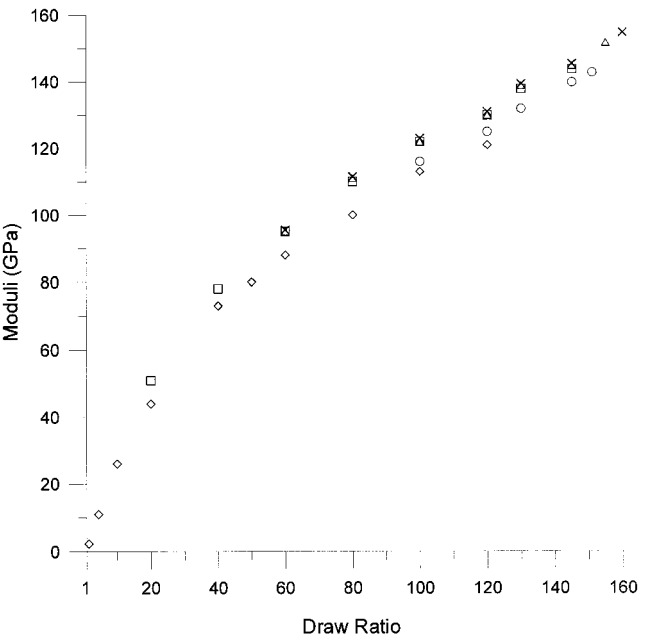

Figure 13 The moduli of (◇) one- and two-stage drawn UL_{10} fiber specimens drawn at their optimum T_{sec} with a D_{lr} of (□) 10, (△) 40, (×) 50, and (○) 80.

The birefringence values, tensile strengths, and moduli of one- and two-stage drawn UL_{10} fiber specimens consistently increase with increasing draw ratios, although the increasing rate of these values is gradually reduced as the draw ratios become greater than certain values. In contrast, at a fixed draw ratio, the two-stage drawn UL_{10} specimens drawn at a higher T_{sec} always exhibit higher birefringence, tensile strengths, and moduli values than those with the same D_{lr} but drawn at a lower T_{sec}. Moreover, at a fixed draw ratio, the birefringence, tensile strengths, and moduli of the fiber specimens drawn at a fixed optimum T_{sec} reached the maximum when they are first drawn up to an optimum D_{lr} of about 50. These results suggest that good orientation of UHMWPE molecules along the drawing direction has a beneficial influence on the tensile strengths and moduli of the fiber specimens, which can be obtained by drawing the fiber specimens using their corresponding optimum T_{sec} and D_{lr}. In fact, by using the proper optimum T_{sec} and D_{lr}, the tensile strengths and moduli of the two-stage drawn UL_{10} fiber specimen can reach more than 11 and 155 GPa, respectively.

The authors express their appreciation to the National Science Council for their support of this work.

References

1. Kajiwara, K.; Mcintyre, J. E. Advanced Fiber Spinning Technology; Woodhead Publishing Ltd.: Cambridge, U.K., 1994; p. 174.

2. Smith, P.; Lemstra, P. J. Macromol Chem 1979, 180, 2983.
3. Kalb, B.; Pennings, A. J. J Mater Sci 1980, 15, 2548.
4. Smith, P.; Lemstra, P. J. J Mater Sci 1980, 15, 505.
5. Tech Text Inte 1996, 4, 3.
6. Sawatari, C.; Okumura, T.; Matsuo, M. Polym J 1986, 18, 741.
7. Darras, D.; Sequela, R.; Rietsch, F. J Polym Sci Part B: Polym Phys 1992, 30, 349.
8. Yeh, J. T.; Chang, S. S. J Mater Sci 2000, 35, 3227.
9. Yeh, J. T.; Chang, S. S.; Yen, M. S. J Appl Polym Sci 1998, 70, 149.
10. Yeh, J. T.; Chang, S. S. Polym Eng Sci 2002, 42, 1558.
11. Yeh, J. T.; Chang, S. S. J Appl Polym Sci 2001, 79, 1890.
12. Yeh, J. T.; Lin, Y. L.; Fan-Chiang, C. C. Macromol Chem Phys 1996, 197, 3531.
13. Yeh, J. T.; Wu, H. C. Polym J 1998, 30, 1.
14. Yeh, J. T.; Lin, Y. T.; Chen, K. N. Polym Eng Sci, to appear.
15. Yeh, J. T.; Lin, Y. T.; Chen, K. N. J Polym Res, to appear.
16. Smith, P.; Chanzy, H. D.; Rotzinger, B. P. Polym Commun 1985, 26, 258.
17. Smith, P.; Chanzy, H. D.; Rotzinger, B. P. J Mater Sci 1987, 22, 523.
18. Matsuo, M.; Sawatari, C.; Iida, M.; Yoneda, M. Polym J 1985, 17, 1197.
19. Kanamoto, T.; Tsurta, A.; Tanana, K.; Takeda, M.; Porter, R. S. Macromolecules 1988, 21, 470.
20. Smook, J.; Pennings, A. J. J Appl Polym Sci 1982, 27, 2209.
21. Ohta, T. Polym Eng Sci 1983, 23, 697.
22. Abo, M. I.; Maaty, E. I.; Olley, R. H.; Bassett, D. C. J Mater Sci 1999, 34, 1975.
23. Mastuo, M.; Sawatari, C.; Nakano, T. Polym J 1986, 18, 759.
24. Cha, W. I.; Hyon, S. H.; Ikada, Y. J Polym Sci Part B: Polym Phys 1994, 32, 297.
25. Yamaura, K.; Tanigami, T.; Hayashi, N.; Kosuda, K. I.; Okuda, S.; Takemura, Y.; Itoh, M.; Matsuzawa, S. J Appl Polym Sci 1990, 40, 905.
26. Yamaura, K.; Suzuki, M.; Yamamoto, M.; Shimada, R.; Tanigami, T. J Appl Polym Sci 1995, 58, 1787.
27. Prevorsek, D. C. Polymer Liquid Crystals; Academic: New York, 1982; p 357.
28. Kalb, B.; Pennings, A. J. Polymer 1980, 21, 3.
29. Wilding, M. A.; Word, I. M. Polymer 1978, 19, 969.
30. Smith, P.; Lemstra, P. J. Polymer 1980, 21, 1341.
31. Kavesh, S.; Prevorsek, D. C. U.S. Pat. 4, 536, 536, 1985.
32. Kavesh, S.; Prevorsek, D. C. U.S. Pat. 4, 551, 296, 1985.
33. Kavesh, S.; Prevorsek, D. C. U.S. Pat. 4, 413, 110, 1983.
34. High Perform Text 1996, 8, 3.
35. Wunderlich, B. Macromolecule Physics; Academic: New York, 1973; Vol. 1, p 338.
36. Roberts, R. C. J Polym Sci 1970, 8, 381.
37. Holdsworth, P. J.; Turner-Jones, A. Polymer 1971, 12, 195.
38. Sweet, G. E.; Bell, J. P. J Polym Sci A-2 1971, 10, 1273.
39. Lin, S. B.; Koenig, J. L. J Polym Sci Polym Phys Ed 1983, 21, 2365.
40. Lin, S. B.; Koenig, J. L. J Polym Sci Polym Symp 1984, 71, 121.
41. Groeninckx, G.; Reynaers, H. J Polym Sci Polym Phys Ed 1980, 18, 1325.
42. Fontaine, F.; Ledent, J.; Groeninckx, G.; Reynaers, H. Polymer 1982, 23, 185.